Acta Oceanol. Sin., 2018, Vol. 37, No. 9, P. 41–49
DOI: 10.1007/s13131-018-1206-4
http://www.hyxb.org.cn
E-mail: hyxbe@263.net

A new global gridded sea surface temperature product constructed from infrared and microwave radiometer data using the optimum interpolation method

SUN Weifu[1], WANG Jin[2]*, ZHANG Jie[1], MA Yi[1], MENG Junmin[1], YANG Lei[3], MIAO Junwei[4]

[1] The First Institute of Oceanography, State Oceanic Administration, Qingdao 266061, China

[2] College of Physics, Qingdao University, Qingdao 266071, China

[3] School of Geosciences, China University of Petroleum (East China), Qingdao 266580, China

[4] College of Geomatics, Shandong University of Science and Technology, Qingdao 266590, China

Received 2 November 2017; accepted 23 January 2018

Abstract

A new 0.1° gridded daily sea surface temperature (SST) data product is presented covering the years 2003–2015. It is created by fusing satellite SST data retrievals from four microwave (WindSat, AMSR-E, ASMR2 and HY-2A RM) and two infrared (MODIS and AVHRR) radiometers (RMs) based on the optimum interpolation (OI) method. The effect of including HY-2A RM SST data in the fusion product is studied, and the accuracy of the new SST product is determined by various comparisons with moored and drifting buoy measurements. An evaluation using global tropical moored buoy measurements shows that the root mean square error (RMSE) of the new gridded SST product is generally less than 0.5°C. A comparison with US National Data Buoy Center meteorological and oceanographic moored buoy observations shows that the RMSE of the new product is generally less than 0.8°C. A comparison with measurements from drifting buoys shows an RMSE of 0.52–0.69°C. Furthermore, the consistency of the new gridded SST dataset and the Remote Sensing Systems microwave-infrared SST dataset is evaluated, and the result shows that no significant inconsistency exists between these two products.

Key words: sea surface temperature, radiometer, data fusion, optimum interpolation

Citation: Sun Weifu, Wang Jin, Zhang Jie, Ma Yi, Meng Junmin, Yang Lei, Miao Junwei. 2018. A new global gridded sea surface temperature product constructed from infrared and microwave radiometer data using the optimum interpolation method. Acta Oceanologica Sinica, 37(9): 41–49, doi: 10.1007/s13131-018-1206-4

1 Introduction

Sea surface temperature (SST) is a key indicator for changes in the earth's climate system (Kawai and Wada, 2007). Thus, accurate knowledge of the SST is essential for climate monitoring, research, and prediction. The SST is also used to define surface boundary conditions for numerical weather prediction and for other atmospheric simulations. Currently, SST-observing satellite missions mainly include two types: microwave radiometers (RMs), such as WindSat and the Advanced Microwave Scanning Radiometer for Earth Observing System (AMSR-E), and infrared RMs, represented by the Moderate Resolution Imaging Spectroradiometer (MODIS) and Advanced Very High Resolution Radiometer (AVHRR). Typical satellite microwave RMs have the ability to penetrate cloud cover and observe the SSTs during any weather, but their large antenna footprint leads to low spatial resolution of the satellite data (Wang et al., 2010). Near coasts and the edges of sea ice, microwave RM observations are affected by microwave radiation from the land and sea ice, respectively, and the data quality is poor. In contrast, infrared RM SST measurements have high spatial resolution, with a typical value of 250 m, but infrared observations are affected by weather conditions, such as cloud and fog, and their spatial coverage is limited. Since both observation methods have drawbacks, the fusion of infrared and microwave RM data is an effective method for creating an SST dataset product with large scale and high spatial resolution.

In recent decades, a variety of SST products have been constructed from satellite-derived SSTs using different statistical methods. Various multiple-satellite SST products were generated; for example, Li et al. (2013) used Bayesian maximum entropy, a nonlinear geo-statistical methodology, to produce 8 d average and spatially continuous SST datasets with 4 km spatial resolution from the MODIS and AMSR-E data. A number of different research institutions, such as the US National Oceanic and Atmospheric Administration (NOAA), U.K. Met Office, US Jet Propulsion Laboratory, Japan Meteorological Agency (JMA), and the Remote Sensing Systems (RSS) Company, have developed SST fusion products. Such products include the Met Office's Operational Sea Surface Temperature and Sea Ice Analysis (OSTIA) System (Martin et al., 2012), the US Naval Oceanographic Office K10 analysis, the JMA merged SST dataset (Chao et al., 2009), and the RSS optimal interpolation (OI) SST product (Xie et al., 2008). The spatial resolution of these SST data products is generally 0.05°–0.25°, and the time resolution is generally daily. However,

Foundation item: The National Key Research and Development Program of China under contract No. 2016YFA0600102; the Basic Scientific Fund for National Public Research Institutes of China under contract No. 2015T03; the State Oceanic Administration's Second Remote Sensing Survey of East India Ocean Environmental Parameters under contract No. GASI-02-IND-YGST$_2$-04.
*Corresponding author, E-mail: feiyu_wj@163.com

no HY-2A RM SST data are used in these products, so the potential application of the new HY-2A RM should be explored and proved.

This paper describes the development of an SST product using data from six satellite-borne instrument sets: four microwave RMs—WindSat, AMSR-E, Advanced Microwave Scanning Radiometer 2 (AMSR2) and HY-2A RM, and two infrared RMs—AVHRR and MODIS. The new SST product covers the years 2003–2015 and has a 0.1° grid of daily observations; data fusion was performed based on the OI method. The new gridded SST dataset was validated using *in situ* data from moored and drifting buoys, as well as the RSS microwave-infrared (MW-IR) SST dataset. Section 2 briefly reviews the satellite SST retrievals and the validation datasets. The OI method and the resulting gridded SSTs are discussed in Section 3. Validation of the new gridded SST dataset is presented in Section 4. The principal conclusions of this paper are summarized in Section 5.

2 Data

2.1 *Satellite data retrievals*

Satellite microwave and infrared RMs are the primary technical tools for global SST remote sensing, and collectively they provide global coverage suitable for SST data fusion. This section describes the SST retrievals from January 1, 2003 to December 31, 2015 that were used in the new SST product. WindSat, ASMR-E, AMSR2, and HY-2A RM, which are onboard polar-orbit satellites covering the global ocean, were selected as sources of microwave RM data. In consideration of the desired high spatial resolution and global ocean coverage of this SST product, AVHRR and MODIS were selected as sources of infrared RM data. All of the sensors used in this paper are described in Fig. 1 and Table 1. Statistical analysis indicated that the combined SST records of the four microwave sensors generally cover over 60% of the global ocean, while the infrared records cover only around 10%. The following paragraphs summarize each sensor's characteristics.

WindSat was the first satellite-based multi-frequency polarimetric microwave RM designed by the US Naval Research Laboratory. It has the ability to observe SSTs with 6.9 GHz and 10.7 GHz channels. RSS provides a WindSat SST daily data product that is divided into ascending and descending swaths with a spatial resolution of 0.25°. The accuracy of the data is about 0.71°C, as determined by comparison with moored buoy data from the US National Data Buoy Center (NDBC) (Zhu et al., 2016).

The AMSR-E is onboard the Aqua satellite developed by the Japan Aerospace Exploration Agency. This RM was in orbit for nearly 10 years, but it stopped rotating on October 4, 2011, owing to an antenna problem (Høyer, 2012). RSS provides ASMR-E SST daily data for a 0.25° grid divided into two maps based on ascending and descending passes. The accuracy of the data is about 0.75°C, as determined by comparison with drifting buoy data (Li et al., 2010).

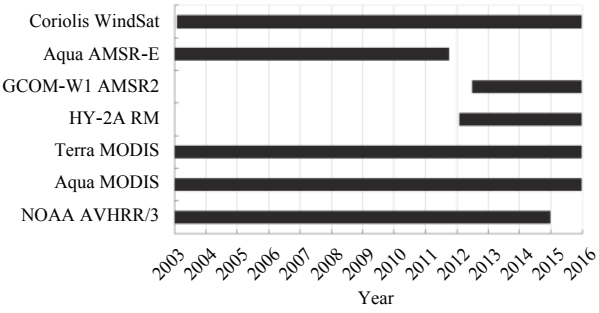

Fig. 1. Temporal coverage of satellite sensors used in the new SST product.

The AMSR2, onboard Japan's Global Change Observation Mission-Water 1 (GCOM-W1) spacecraft, is the successor to AMSR-E. It launched in May 2012 to ensure the continuity of SST data (Zabolotskikh et al., 2014). AMSR2 can provide highly accurate measurements of SSTs at low-frequency channels of 6.9 GHz, 7.3 GHz and 10.65 GHz. RSS provides ASMR2 SST daily data with a data resolution about the same as that of the ASMR-E microwave RM. The accuracy of the data is about 0.56°C, as determined by comparison with Global Telecommunication System buoy data.

The HY-2A satellite is China's first ocean dynamic environment satellite, and it carries four microwave instruments for all-weather observation of dynamic global ocean environment parameters. Oceanic and atmospheric parameters, such as SST, wind speed, and water vapor and liquid content, can be obtained by its onboard RM (Jiang et al., 2012). The SST data are produced by the China National Satellite Ocean Application Service. The accuracy of the data is about 1.7°C, as determined by comparison with the moored buoy data from the international Tropical Atmosphere Ocean (TAO) Array and NDBC (Zhao, 2014).

The MODIS is an infrared RM onboard the Terra and Aqua satellites, which are both currently in normal operation (Hosoda and Qin, 2011). The US National Aeronautics and Space Administration (NASA) produces MODIS 4 km/daily SST data, which are available on NASA's OceanColor Web. The accuracy of the data is about 0.43°C, as determined by comparison with ship observations (Barton and Pearce, 2006).

The AVHRR is an instrument package onboard a series of satellites designed by the NOAA (Shaw and Vennell, 2000). The instruments are often used to image cloud cover and retrieve the SSTs. The US National Centers for Environmental Information produces the AVHRR 4 km/daily SST data, and the data grid is the same as that for the MODIS. The accuracy of the data is about

Table 1. Sensors used in the new SST product

Sensor	Data time used	Local time	SST resolution
Coriolis WindSat	2003.02.05–2015.12.31	6:00/18:00	Daily/25 km
Aqua AMSR-E	2003.01.01–2011.10.04	1:30/13:30	Daily/25 km
GCOM-W1 AMSR2	2012.07.02–2015.12.31	1:30/13:30	Daily/25 km
HY-2A RM	2012.02.07–2015.12.31	6:00/18:00	Swath/97 km
Terra MODIS	2003.01.01–2015.12.31	10:30	Daily/4 km
Aqua MODIS	2003.01.01–2015.12.31	13:30	Daily/4 km
NOAA-17 AVHRR/3	2003.01.01–2005.12.31	10:00	Daily/4 km
NOAA-18 AVHRR/3	2006.01.01–2010.12.31	14:00	Daily/4 km
NOAA-19 AVHRR/3	2011.01.01–2014.12.31	14:00	Daily/4 km

0.68°C, as determined by comparison with TAO observations (Barton and Pearce, 2006).

2.2 *SST background*

The SST background field is used to establish first-guess values for SST fusion. The European Centre for Medium-Range Weather Forecasts (ECMWF) provides European reanalysis (ERA) interim 1°/daily SSTs four times per day (at 00:00:00, 06:00:00, 12:00:00, and 18:00:00). In this study, the four ERA data points were used to generate a daily average SST as the first-guess field.

2.3 *In situ data*

Buoy measurements were obtained to validate the new gridded SSTs. During the 13 a period covered by this study, more than 200 moored buoys and more than 3 000 drifting buoys were operating in the global ocean.

(1) Global tropical moored buoy measurements. The Global Tropical Moored Buoy Array is a multi-national effort to provide data in real time for climate research and forecasting. Major components include the TAO Array in the Pacific (McPhaden et al., 1998), the Prediction and Research Moored Array in the Tropical Atlantic (PIRATA) (Bourlès et al., 2008), and the Research Moored Array for African-Asian-Australian Monsoon Analysis and Prediction (RAMA) in the Indian Ocean (McPhaden et al., 2009). The moored buoys are distributed in tropical and subtropical waters within 30°N to 30°S, where the water temperature is generally stable above 20°C. This study validated the new SST product using observations provided by 67 TAO buoys, 27 RAMA buoys, and 18 PIRATA buoys. These data are freely available from the NOAA for research. First, buoy data were preprocessed to filter out bad or low-quality measurements. Then the daily averaged SSTs were compared with the new gridded SSTs. Tropical moored buoy locations are shown in Fig. 2.

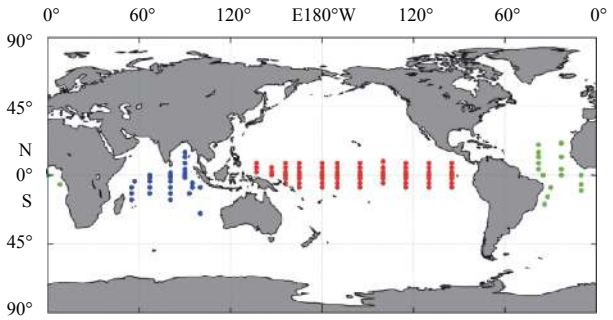

Fig. 2. Global tropical moored buoy locations (blue: RAMA, red: TAO, green: PIRATA).

(2) NDBC meteorological and oceanographic moored buoy measurements. The NDBC manages the development, operation, and maintenance of the national data buoy network. It serves as NOAA's focal point for data buoys and associated meteorological and environmental monitoring technology. The NDBC provides high-quality meteorological and oceanographic data in real time from automated observation systems that include moored buoys and the Coastal-Marine Automated Network in US coastal zones. While the global tropical moored buoy measurements described above were used to validate the SST accuracy for the open ocean, more than 100 NDBC moored buoys surrounding the United States were used to validate the fusion SSTs in coastal zones. The NOAA provides these data freely. The NDBC meteorological and oceanographic moored buoy locations are shown in Fig. 3.

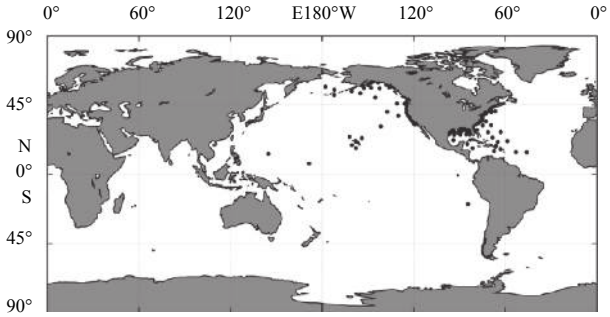

Fig. 3. NDBC meteorological and oceanographic moored buoy locations (black spots).

(3) Drifting buoy measurements. The international Array for Real-time Geostrophic Oceanography (Argo), completed in November 2007, is a global array of more than 3 000 free-drifting profiling floats that measure the temperature profile from the sea surface to a depth of 2 000 m. This allows, for the first time, continuously monitored temperatures to be made publicly available within hours of collection. The buoys of the Argo observation network were placed to form a 3° × 3° grid. One complete measurement cycle (depth profile) takes 10–14 d, so the time resolution of the measurement data is low. The data are provided in NetCDF format by the Global Ocean Data Assimilation Experiment. The Argo buoys cover the global ocean, and the range of the SST data is far greater than that of the TAO array and other moored buoys. Thus, the Argo data can test the accuracy of the new SST product in the global ocean. In this study, the Argo SST measurements closest to the sea surface (depth of about 5 m) were chosen as the SST *in situ* data, and a quality control was performed on these data to remove the poor-quality measurements according to the data flag in each file. The coverage of the Argo SST observations is shown in Fig. 4.

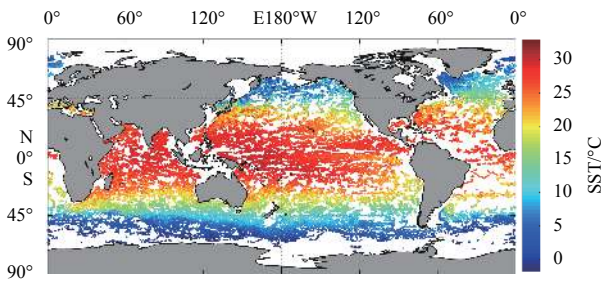

Fig. 4. SST observations by Argo.

2.4 *RSS fusion data*

The RSS MW-IR SST dataset from June 2002 to the present is created using both microwave and infrared SST data. The microwave SST retrievals include data from the Tropical Rainfall Measuring Mission Microwave Imager, the AMSR-E, the AMSR2, and the WindSat, and the infrared SST retrievals include data from the Terra MODIS and the Aqua MODIS. Compared with the Argo buoy observations in the South China Sea and adjacent waters during the years 2008 and 2009, the statistical results show that the root mean square error (RMSE) of the RSS MW-IR

product is about 0.4, whereas the bias has a negative value of –0.06 (Hu et al., 2015). Each binary SST data file available from the RSS consists of three two-dimensional data arrays consisting of (1) single-byte values representing a given day's SSTs, (2) interpolation error estimates, and (3) data masking information. The size of the RSS MW-IR SST dataset is 4 096 by 2 048, which corresponds to a spatial resolution of a grid of approximately 9 km. In this study, the RSS MW-IR SSTs were used to analyze the consistency of the new gridded SSTs because of the similar spatial resolution between the two SST datasets.

3 SST fusion product development

Currently, available SST data fusion algorithms mainly include the following: successive correction method (Wang et al., 2000), blended analysis method (Reynolds and Marsico, 1993), objective analysis method (Wu et al., 1999; Guan and Kawamura, 2004), wavelet transform method (Zhang, 2006), Kriging interpolation method (Song, 2011), Kalman filter method (Wang et al., 2010), and OI method (Reynolds and Smith, 1994; Reynolds et al., 2002, 2007; Xi, 2011). Most of these methods have drawbacks. The successive correction method, which uses the background field and current observation data, leads to poor timeliness owing to the lack of measured SST data. The blended analysis method using in-situ and satellite data is suitable for generating monthly average SSTs because of the limitations of measured SST data. Depending on the SST accuracy and spatial resolution, the objective analysis method using the SST data from one of the various satellites in each temporal series and spatial field may generate singular values. The wavelet transform method easily causes boundary distortion and results in low SST precision. The Kriging interpolation result is unstable if an insufficient number of data points are around the interpolation position. The Kalman filter method can generate the SSTs with high precision and spatial resolution, but it has a large number of calculations. Thus, this method takes a long time to produce the global ocean SSTs. The OI method has fewer calculations than the Kalman filter method, and its SST product has high precision and global coverage. Therefore, the OI method can generate a long time series of high-precision global ocean SSTs for climate studies. For these reasons, the OI method is the most widely used the SST fusion algorithm, and it is used in products such as the RSS MW-IR SST, Reynolds SST analysis, and OSTIA Systems datasets.

3.1 *OI method*

As discussed above, the satellite SST sensors have different resolutions and accuracies, and none of them can cover 100% of the global ocean in 24 h. It is difficult to use these satellite SST datasets, with their many data gaps, to analyze the spatial-temporal variation of the global ocean SST over a long time series and explain the phenomena and processes of the global climate change. Thus, the OI is a widely used method in oceanography and meteorology to make use of the statistical properties of irregularly spaced data (in time and space) to interpolate the data onto a regularly sampled grid. The generalized interpolation expression is as follows:

$$A_k = B_k + r_k, \tag{1}$$

where $A_k(B_k)$ is the analysis (first guess) value at analysis grid cell k; and r_k is the analysis increment, which is the difference between the analysis and the first-guess SST. The increment r_k can be determined by the following equation:

$$r_k = \sum_{i=1}^{N} w_{i,\,k}\,(O_i - B_i)\,, \tag{2}$$

where O_i is the observed value; B_i is the first-guess value; $w_{i,\,k}$ is the weight function at observation point i; k is the analysis grid point; and N is the number of observation points. The weight was formally defined by Reynolds and Smith (1994). Here the ensemble average of the analysis correlation error $\langle \pi_i \pi_j \rangle$ is assumed to be Gaussian and is expressed as

$$\langle \pi_i \pi_j \rangle = \exp\left[\frac{-(x_i - x_j)^2}{\lambda_x^2} + \frac{-(y_i - y_j)^2}{\lambda_y^2}\right], \tag{3}$$

where x and y are the zonal and meridional locations of grid points i and j, respectively; and λ_x and λ_y are the zonal and meridional spatial scales. Here, λ_x and λ_y were set to 151 and 155 km, respectively. The weights can then be determined as follows:

$$\sum_{i=1}^{N} \left(\langle \pi_i \pi_j \rangle + \varepsilon_i^2 \delta_{i,j}\right) w_{i,k} = \langle \pi_j \pi_k \rangle\,, \tag{4}$$

where ε_i is the noise-to-signal standard deviation ratio, which needs to be determined as 0.5 (Reynolds and Smith, 1994; Reynolds et al., 2007). The ensemble averages of the data errors are assumed to be uncorrelated between different observations. Thus, the data correlation error is $\delta_{i,\,j}$=1 for i=j and $\delta_{i,\,j}$=0 for all other cases.

Note that the actual SSTs only appear in Eq. (2). The remaining equations to determine the weights depend only on the distance via Eq. (3) and noise-to-signal ratios for the available SST data. The set of linear equations defined by Eq. (4) is solved at each grid point k.

3.2 *SST fusion process*

Because the SSTs from the various RMs have different resolutions, a series of preprocesses were needed before the fusion procedure could be performed. The range of –3 to 40°C was chosen for the effective values of microwave and infrared SST retrievals, and valid data were also delineated using the quality flags. The process flow is shown in Fig. 5. First, the background was interpolated onto a 0.04° grid for the infrared SST retrievals, a 0.25° grid for the microwave SST retrievals, and a 0.1° grid for the fusion SSTs. Then, based on the new 0.04° and 0.25° background and corresponding SST retrievals, the increments (O_i–B_i) were

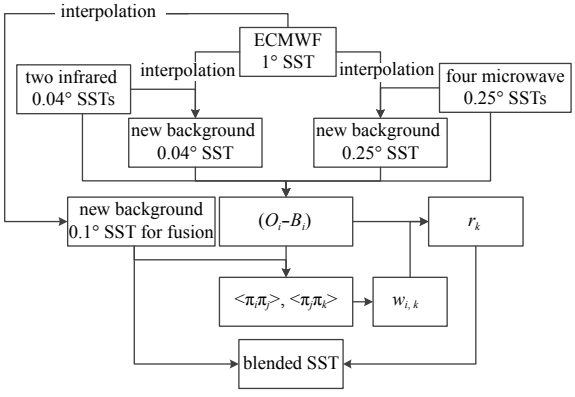

Fig. 5. SST fusion process.

calculated. After that, $w_{i,k}$ and r_k were also obtained using the increments. Finally, using the previous calculation results, the new 0.1° gridded SSTs were calculated.

3.3 *SST fusion based on the OI method*

On the basis of the OI method, the new global ocean gridded SST data from 2003 to 2015 were blended using the WindSat, AMSR-E, ASMR2, HY-2A RM, MODIS (Aqua/Terra), and AVHRR SST retrievals. To explore the quality influence of the HY-2A RM on the fusion results, the new global ocean gridded SSTs not using the HY-2A RM data were also blended for 2012–2015. The time resolution of the SSTs is daily, the spatial resolution is 0.1°, and the product format is NetCDF. The new gridded SST sample data for January 1, 2012 are shown in Fig. 6.

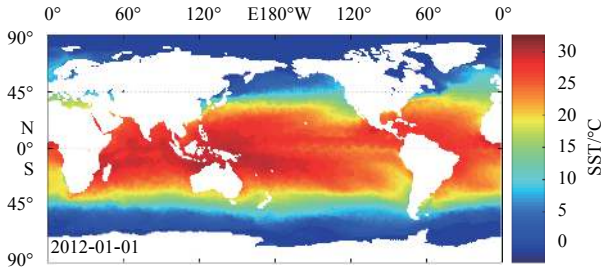

Fig. 6. New SST sample data for January 1, 2012 based on OI.

4 SST validation

In this section, first, the quality influence of HY-2A RM SST data on the fusion product is discussed to confirm the appropriateness of including the HY-2A RM SST retrievals. Then, using in-situ data from tropical moored buoys (TAO, RAMA and PIRATA), NDBC meteorological and oceanographic moored buoys, and drifting buoys (Argo), the accuracy of the new gridded SSTs is assessed. The SSTs were also compared with the RSS MW-IR SSTs for further validation. Temporal-spatial matching was performed and then statistical parameters, such as mean bias, RMSE, and correlation coefficient, were calculated to characterize the differences between the buoy measurements and new gridded SSTs and RSS SST data and new gridded SSTs during the period 2003–2015.

(1) Fusion product quality analysis with and without HY-2A RM data. To explore the quality influence of the HY-2A RM data on the data fusion product, the study compared two new fusion products: one using HY-2A RM data and another that did not use these data. Both fusion products used the same SSTs from RMs other than HY-2A RM and blended them employing the same OI algorithm, but the study only used the Argo buoy observations covering the global ocean to make the comparison. Each fusion product was compared with the Argo buoy observations using limits in the given temporal and spatial windows of 24 h and 50 km. The resulting mean bias, the RMSE, and the correlation coefficient are shown in Table 2. The results show that the mean bias and the RMSE increased slightly (<10%) when the HY-2A RM SSTs were used, and this increase was small enough to be ignored.

The influence of the HY-2A RM data on the global ocean SST coverage was also studied using four combinations of datasets for 2013: AMSR2 plus WindSat (A), A plus HY-2A RM (B), A plus MODIS plus AVHRR (C), and C plus HY-2A RM (D). The spatial coverage of these different dataset combinations is shown in Fig. 7. The results show that the HY-2A RM data can increase the spatial coverage by 7% when the microwave data are used and by 6% when both microwave and infrared data are used. Thus, inclusion of the SSTs retrieved by the HY-2A RM can improve the spatial coverage of the global ocean SSTs, and in the following sections, the new gridded SSTs include the HY-2A RM retrievals in the data fusion.

(2) Comparison with global tropical moored buoy observations. To compare the new gridded SSTs with moored buoy measurements, a spatial and temporal collocation was performed between the two datasets. The new gridded SSTs and buoy data pairs were collocated within a grid window of 50 km and a time interval between buoy measurements of 24 h. A match-up dataset was constituted after matching between the new gridded SSTs and moored buoy data. The mean bias, RMSE, and correlation coefficient of the new gridded SSTs were calcu-

Table 2. Fusion SST quality analysis with and without HY-2A RM data for 2012–2015

Year	Mean bias/°C		RMSE/°C		Correlation coefficient	
	With	Without	With	Without	With	Without
2012	–0.10	–0.07	0.60	0.56	0.99	0.99
2013	–0.12	–0.07	0.57	0.52	0.99	0.99
2014	–0.04	0.02	0.57	0.53	0.99	0.99
2015	–0.01	–0.01	0.59	0.56	0.99	0.99

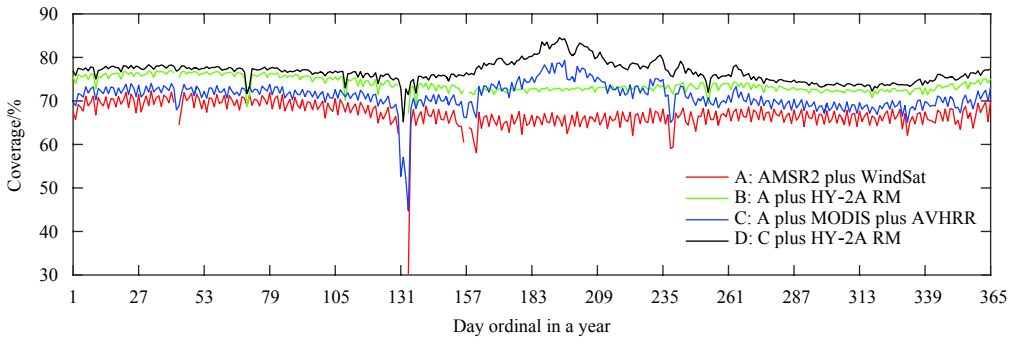

Fig. 7. Spatial coverage of global ocean SST using different dataset combinations.

Table 3. Comparison between new gridded SST and moored buoy data for 2003–2015

Year	Data matched	Mean bias/°C	RMSE/°C	Correlation coefficient
2003	22 917	–0.16	0.46	0.97
2004	22 217	–0.14	0.43	0.98
2005	22 193	–0.23	0.51	0.97
2006	22 991	0.05	0.44	0.97
2007	25 248	–0.19	0.46	0.98
2008	26 829	0.04	0.41	0.97
2009	27 240	–0.08	0.37	0.98
2010	28 001	–0.07	0.39	0.98
2011	29 836	–0.11	0.35	0.98
2012	22 906	–0.17	0.43	0.98
2013	18 143	–0.19	0.42	0.98
2014	18 507	–0.07	0.36	0.99
2015	28 322	–0.06	0.37	0.98

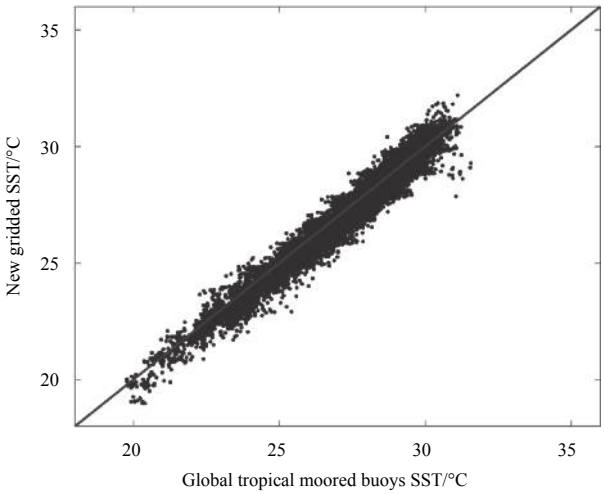

Fig. 8. Scatter plot for new fusion SSTs and global tropical moored buoy data.

lated, the results of which are shown in Table 3. The scatter chart for the new gridded SST assessment is plotted in Fig. 8. The results show that the new gridded SSTs have a negative bias and the RMSE is generally less than 0.5°C.

(3) Comparison with NDBC meteorological and oceanographic moored buoy observations. The *in situ* buoy data from 2003 and 2004 were too scarce to support precise verification with a 50 km grid and 24 h time interval. Therefore, the data from these 2 a were excluded from this validation. The mean bias, RMSE, and correlation coefficient of the new SSTs were calculated for 2005–2015, as shown in Table 4. The scatter chart of the new gridded SST assessment is plotted in Fig. 9. The results show that the RMSE is generally less than 0.8°C, which is slightly higher than the results from comparison with global tropical moored buoy observations. The main cause may be contamination by land radio-frequency interference, which can affect the accuracy of microwave SST data.

(4) Comparison with drifting buoy observations. This comparison was conducted using temporal and spatial windows of 24 h and 50 km, respectively. The mean bias, RMSE, and correlation coefficient of the new SSTs were calculated, as shown in Table 5. The scatter chart of the new gridded SSTs is plotted in Fig. 10. The table shows that, as the number of Argo buoys increases, the number of effective data matches also increases. The new gridded SSTs obtained in this study have a negative deviation of about –0.1°C in most years, and the RMSE is relatively stable with a value of 0.52–0.69°C.

(5) Consistency with RSS MW-IR SST dataset. The consistency of the new gridded SSTs and the RSS MW-IR SSTs was evaluated for the period 2010–2015. First, the RSS MW-IR SSTs were interpolated onto a 10 km (0.1°) grid. Then, the mean bias and the RMSE were calculated, as shown in Table 6.

As shown in Table 6, the mean bias is stable and near 0, and the RMSE is generally about 0.7°C. To further illustrate the global distributions of the bias and the RMSE, Fig. 11 provides a global map of the bias and the RMSE for 2014. As shown in Fig. 11, over most of the global ocean, the bias is generally about 0 and the RMSE is generally less than 0.8°C. The largest RMSE between the two SST products appears in the north polar and sub polar seas,

Table 4. Comparison between new SSTs and NDBC moored buoy data for 2005–2015

Year	Data matched	Mean bias/°C	RMSE/°C	Correlation coefficient
2005	11 937	–0.16	0.76	0.99
2006	13 515	0.06	0.82	0.99
2007	13 133	–0.11	0.77	0.99
2008	14 593	0.09	0.79	0.99
2009	14 716	0.03	0.79	0.99
2010	13 836	0.06	0.87	0.99
2011	12 842	0.02	0.65	0.99
2012	16 918	–0.05	0.63	0.99
2013	16 038	–0.08	0.63	0.99
2014	17 484	–0.01	0.60	0.99
2015	19 939	0.01	0.60	0.99

Table 5. Comparison between new SSTs and Argo buoys for 2003–2015

Year	Data matched	Mean bias/°C	RMSE/°C	Correlation coefficient
2003	16 267	–0.11	0.67	0.99
2004	22 302	–0.12	0.64	0.99
2005	36 841	–0.17	0.69	0.99
2006	54 815	–0.02	0.67	0.99
2007	66 814	–0.16	0.59	0.99
2008	75 342	0.07	0.60	0.99
2009	76 423	–0.01	0.54	0.99
2010	77 347	0.03	0.62	0.99
2011	85 402	–0.06	0.52	0.99
2012	94 633	–0.10	0.60	0.99
2013	101 680	–0.12	0.57	0.99
2014	102 048	–0.04	0.57	0.99
2015	102 060	–0.01	0.59	0.99

Table 6. Consistency between new SST and RSS SST for 2010–2015

Year	Data matched	Mean bias/°C	RMSE/°C	Correlation coefficient
2010	1.22×10^9	0.004	0.66	0.99
2011	1.23×10^9	–0.040	0.60	0.99
2012	1.23×10^9	–0.010	0.68	0.99
2013	1.23×10^9	–0.040	0.73	0.99
2014	1.21×10^9	0.130	0.70	0.99
2015	1.22×10^9	0.140	0.72	0.99

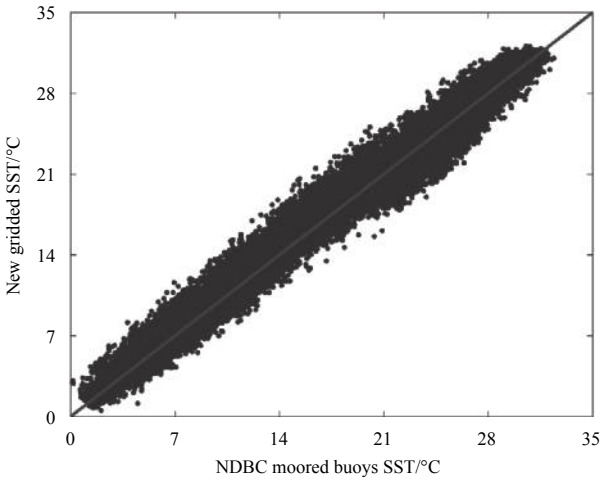

Fig. 9. Scatter plot for new fusion SSTs and NDBC moored buoy data.

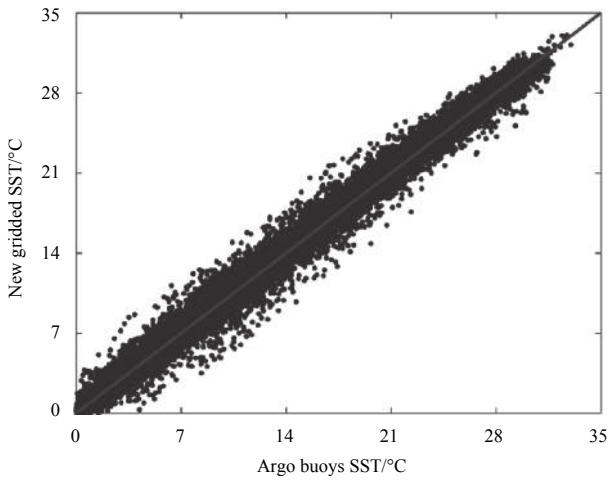

Fig. 10. Scatter plot for new SSTs and Argo buoy data.

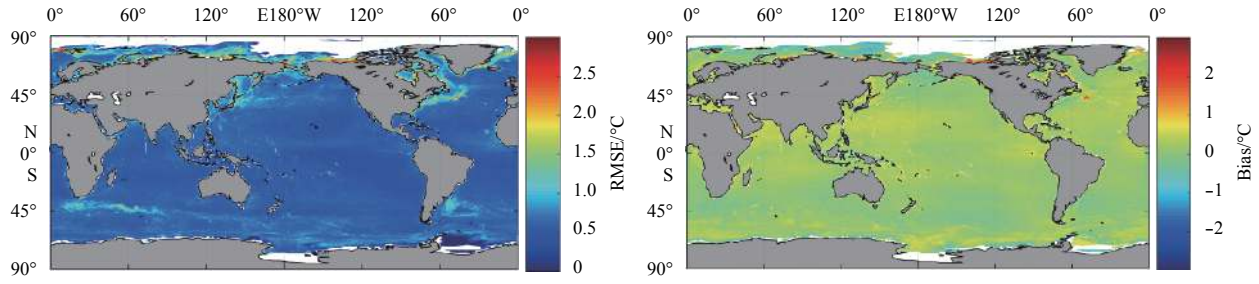

Fig. 11. Global distributions of the RMSE and bias.

followed by US coastal regions; the smallest RMSE appears in the south polar seas. Thus, it can be concluded that the new gridded SSTs coincide with the RSS MW-IR SSTs for most of the global ocean, except for some polar and coastal areas. A possible reas-

on for the larger RMSE in these areas is signal contamination from land and sea ice.

5 Conclusions

The SST is one of the most important parameters for studying the global ocean-atmosphere system. As a key factor affecting the marine dynamic environment and ocean-atmosphere interaction, the SST describes the basic physical properties of the ocean. A long-term SST data product can be obtained from two kinds of satellite RMs, infrared and microwave, which have different spatial resolutions and different accuracies. The infrared RMs (such as MODIS and AVHRR) have higher spatial resolution, but they are affected by meteorological conditions. The microwave RMs, such as the WindSat, ASMR-E, AMSR2 and HY-2A RM, have better spatial global coverage, but their spatial resolution is limited.

The SST retrievals by different infrared and microwave RMs make it possible to generate more complete and accurate SST products based on data fusion methods. Using satellite SST retrievals from infrared (MODIS and AVHRR) and microwave (WindSat, AMSR-E, ASMR2 and HY-2A RM) RMs, a new global ocean SST dataset was developed based on the OI method. The new global ocean dataset has a spatial resolution of 0.1° and temporal resolution of 24 h. The influence of HY-2A RM data on the fusion product was evaluated by comparison with Argo buoy data. The HY-2A RM data were found to improve the spatial coverage of dataset without introducing significant error. An evaluation using independent observations from TAO, RAMA, and PIRATA moored buoy SST measurements showed that the RMSE of the new SST dataset is generally less than 0.5°C. Comparison with NDBC meteorological and oceanographic moored buoy observations showed that the RMSE of the new SST dataset is generally less than 0.8°C. By comparison with the measurements from Argo buoys, the RMSE of the new SSTs was found to be 0.52–0.69°C. The consistency of the new gridded SSTs and RSS MW-IR SSTs was also evaluated, and it was found that no significant inconsistency exists between them.

This study showed that the HY-2A RM SST retrievals can be used to generate reliable global gridded SST datasets. Thus, the increased use of the HY-2A RM data is well worth considering and should be further studied. Moreover, the accuracy differences between satellite SST retrievals need to be considered in future research to obtain more accurate SST products.

Acknowledgements

The authors thank RSS, NSOAS, NASA, NOAA, GODAE respectively for providing the SST data of WindSat, AMSR-E, AMSR2, HY-2A RM, MODIS, AVHRR, moored buoys, Argo buoys and RSS WM_IR SSTs.

References

Barton I, Pearce A. 2006. Validation of GLI and other satellite-derived sea surface temperatures using data from the Rottnest Island ferry, Western Australia. Journal of Oceanography, 62(3): 303–310

Bourlès B, Lumpkin R, McPhaden M J, et al. 2008. THE PIRATA program: history, accomplishments, and future directions. Bulletin of the American Meteorological Society, 89(8): 1111–1126

Chao Yi, Li Zhijin, Farrara J D, et al. 2009. Blending sea surface temperatures from multiple satellites and in situ observations for coastal oceans. Journal of Atmospheric and Oceanic Technology, 26(7): 1415–1426

Guan Lei, Kawamura H. 2004. Merging satellite infrared and microwave SSTs: Methodology and evaluation of the new SST. Journal of Oceanography, 60(5): 905–912

Hosoda K, Qin Huiling. 2011. Algorithm for estimating sea surface temperatures based on Aqua/MODIS global ocean data. 1. Development and validation of the algorithm. Journal of Oceanography, 67(1): 135–145

Høyer J L, Karagali I, Dybkjær G, et al. 2012. Multi sensor validation and error characteristics of Arctic satellite sea surface temperature observations. Remote Sensing of Environment, 121: 335–346

Hu Xiaoyue, Zhang Caiyun, Shang Shaoling. 2015. Validation and inter-comparison of multi-satellite merged sea surface temperature products in the South China Sea and its adjacent waters. Journal of Remote Sensing (in Chinese), 19(2): 328–338

Jiang Xingwei, Lin Mingsen, Liu Jianqiang, et al. 2012. The HY-2 satellite and its preliminary assessment. International Journal of Digital Earth, 5(3): 266–281

Kawai Y, Wada A. 2007. Diurnal sea surface temperature variation and its impact on the atmosphere and ocean: A review. Journal of Oceanography, 63(5): 721–744

Li Aihua, Bo Yanchen, Zhu Yuxin, et al. 2013. Blending multi-resolution satellite sea surface temperature (SST) products using Bayesian maximum entropy method. Remote Sensing of Environment, 135: 52–63

Li Ming, Liu Jiping, Zhang Zhanhai, et al. 2010. Evaluation of AMSR-E SST in the Southern Ocean using drifting buoy data. Haiyang Xuebao (in Chinese), 32(6): 47–55

Martin M, Dash P, Ignatov A, et al. 2012. Group for High Resolution Sea Surface temperature (GHRSST) analysis fields inter-comparisons. Part I: A GHRSST multi-product ensemble (GMPE). Deep Sea Research Part II: Topical Studies in Oceanography, 77–80: 21–30

McPhaden M J, Busalacchi A J, Cheney R, et al. 1998. The tropical ocean–global atmosphere observing system: A decade of progress. Journal of Geophysical Research: Oceans, 103(C7): 14169–14240

McPhaden M J, Meyers G, Ando K, et al. 2009. RAMA: The research moored array for African-Asian-Australian monsoon analysis and prediction. Bulletin of the American Meteorological Society, 90(4): 459–480

Reynolds R W, Marsico D C. 1993. An improved real-time global sea surface temperature analysis. Journal of Climate, 6(1): 114–119

Reynolds R W, Rayner N A, Smith T M, et al. 2002. An improved in situ and satellite SST analysis for climate. Journal of Climate, 15(13): 1609–1625

Reynolds R W, Smith T M. 1994. Improved global sea surface temperature analyses using optimum interpolation. Journal of Climate, 7(6): 929–948

Reynolds R W, Smith T M, Liu Chunying, et al. 2007. Daily high-resolution-blended analyses for sea surface temperature. Journal of Climate, 20(22): 5473–5496

Shaw A G P, Vennell R. 2000. A front-following algorithm for AVHRR SST imagery. Remote Sensing of Environment, 72(3): 317–327

Song Qinglei. 2011. Processing of surface temperature data in East China Sea based on Kriging interpolation and effect analysis [dissertation]. Qingdao: The First Institute of Oceanography, State Oceanic Administration

Wang Keguang, Zhang Jianhua, Wang Caixin. 2000. Objective analysis method of conventional SST data in the Northwest Pacific Ocean: I. Analysis of ten day average ship report data. Marine Forecasts (in Chinese), 17(4): 52–59

Wang Yanzhen, Guan Lei, Qu Liqin. 2010. Merging Sea surface temperature observed by satellite infrared and microwave radiometers using Kalman Filter. Periodical of Ocean University of China (in Chinese), 40(12): 126–130

Wu Xiangqian, Menzel W P, Wade G S. 1999. Estimation of sea surface temperatures using *GOES-8/9* radiance measurements. Bulletin of the American Meteorological Society, 80(6): 1127–1138

Xi Meng. 2011. Merging infrared radiometer and microwave radiometer Sea Surface Temperature data based on the optimum interpolation [dissertation]. Beijing: National Marine Environment Forecasting Center

Xie Jiping, Zhu Jiang, Li Yan. 2008. Assessment and inter-comparison of five high-resolution sea surface temperature products in the shelf and coastal seas around China. Continental Shelf Research, 28(10): 1286–1293

Zabolotskikh E, Mitnik L, Reul N, et al. 2014. New possibilities for geophysical parameter retrievals opened by GCOM-W1 AMSR2. IEEE Journal of Selected Topics in Applied Earth Observations and Remote Sensing, 8(9): 4248–4261

Zhang Hui. 2006. Merging AVHRR and AMSR-E sea surface temperature data based on wavelet transform [dissertation]. Qingdao: Ocean University of China

Zhao Yili, Zhu Jianhua, Lin Mingsen, et al. 2014. Assessment of the initial sea surface temperature product of the scanning microwave radiometer aboard on HY-2 satellite. Acta Oceanologica Sinica, 33(1): 109–113

Zhu Enze, Zhang Lei, Shi Hanqing, et al. 2016. Accuracy of WindSat sea surface temperature: Comparison of buoy data from 2004 to 2013. Journal of Remote Sensing (in Chinese), 20(2): 315–327